Evidence of two-stage melting of Wigner solids

Talbot Knighton, Zhe Wu, Jian Huang, Alessandro Serafin, J. S. Xia, L. N. Pfeiffer, and K. W. West

Phys. Rev. B **97**, 085135 — Published 20 February 2018

DOI: 10.1103/PhysRevB.97.085135

Evidence of two-stage melting of Wigner solids

Talbot Knighton, Zhe Wu, and Jian Huang
Department of Physics and Astronomy, Wayne State University, Detroit, MI 48201, USA

Alessandro Serafin and J. S. Xia
National High Field Magnetic Laboratory, Tallahassee, FL 32310

L. N. Pfeiffer and K. W. West
Department of Electrical Engineering, Princeton University, Princeton, NJ 08544
(Dated: January 25, 2018)

Ultra-low carrier concentrations of two-dimensional holes down to $p = 1 \times 10^9$ cm^{-2} are realized. Remarkable insulating states are found below a critical density of $p_c = 4 \times 10^9$ cm^{-2} or $r_s \approx 40$. Sensitive dc *VI* measurement as a function of temperature and electric field reveals a two-stage phase transition supporting the melting of a Wigner solid as a two-stage first-order transition.

A Wigner crystal (WC) [1] of electrons is a long-sought-after phenomenon driven by strong electron-electron interaction and the melting of a WC provides a unique opportunity of understanding the solid-liquid transition (SLT) [2–4]. According to the Monte Carlo calculations, a WC occurs when the ratio of the inter-particle Coulomb energy E_{ee} and the Fermi energy E_F, $r_s = E_{ee}/E_F = a/a_B$, is at least 37 [5]. $a = 1/\sqrt{\pi n}$ is the Wigner-Seitz radius for electron density n and $a_B = \hbar^2\epsilon/m^*e^2$ is the Bohr radius. Therefore, in order to observe a WC, the charge concentrations must be extremely dilute, i.e. $\leq 1 \times 10^9$cm^{-2} for electrons or $\leq 4 \times 10^9$cm^{-2} for holes in GaAs two-dimensional (2D) systems. Experiments in such small electron energy limits are challenging because the disorder effects, unless effective suppressed, easily overwhelm the interaction-driven effects. Natural consequences are the Anderson localization [6], glass states [7], and mixed phases; all of which do not possess true long range correlations. As a result, neither a WC nor a melting transition has been clearly demonstrated. Most detection efforts target collective modes and have so far produced only softly-pinned modes undergoing a second-order-like thermal melting. These modes, as broadly suspected, could easily result from intermediate or mixed phases (e.g. hexatics, bubbles/stripes, or glass phases) since the observed correlation lengths (ξ), corresponding to the sizes of WCs, are usually small. Clear evidence of a WC demands not only demonstrations of longer or even macroscopic ξ, but, moreover, a melting transition marked by a singularity [8–10]. This work presents evidence for collective pinning modes characterized by a macroscopic ξ, as well as two-stage SLT, analogous to the Kosterlitz-Thouless (KT) model [4, 11–16], except for a first-order transition suggested by a discontinuity across the critical point.

Most WC studies adopt the reentrant and quantum Hall insulating phases (RIP&QHIP) in a large magnetic field (B) where interaction effect is enhanced without reaching an ultra-dilute limit. Detection of the collective modes has been conducted with respect to pinning [17–19], and resonant absorption (via rf, microwaves, acoustic waves [20–23], tunneling [24]). However, there lacks evidence distinguishing a WC from intermediate/mixed phases. In fact, the estimated ξ is not only small (up to 1μm), but also decays exponentially with increasing temperature (T) in a fashion similar to what is expected for an intermediate phase (i.e. hexatics [13, 25]). Similar results are also obtained through studies in zero B fields [26–28]. Zero-B results at $r_s > 40$ are quite rare due to the requirement for far more dilute carrier densities where disorder effect is even more prominent because the screening effect is weak as the inter-particle spacing, $a = 1/\sqrt{\pi n} \sim 200 - 500n$m, approaches the screening length. This is why even fairly clean systems become highly insulating when n is $\sim 8 - 9 \times 10^9$cm^{-2} [28, 29]. Consequently, r_s is limited to 5-15. Therefore, disorder suppression, as supported by almost all experiments, remains the key to successful detection of WCs.

In addition to driving a localization, another subtle disorder effect is its influence on the WC melting temperature (T_m), i.e. via fluctuations that break long-range translational symmetry. This less understood effect could alter current models of melting such as the KT model and is expected to be more effective in suppressing T_m than the quantum fluctuations [9, 10]. Disorder suppression is therefore key in keeping T_m accessible. Most reported $T_m \sim 100 - 200$ mK for small ξ cases are likely the crossover points between the intermediate/mixed and the liquid phases. To probe a transition, i.e. from a WC-intermediate phase, requires cooling to lower T.

This study focuses on the dc transport response of collective pinning and melting in ultra-high quality dilute 2D systems. A proven cooling method using a helium-3 immersion cell is adopted [30]. Key observations include enormously pinned collective modes, characterized by a differential resistance (r_d) of $\sim$ 1.3GΩ, that exhibit a remarkable threshold nonlinear dc-IV identical to pinned charge density waves (CDWs). The critical temperature is T_m $\sim$35 mK. Moreover, heating across T_m results in a discontinuity in r_d which supports a first-order two-stage thermal melting. The presentation is divided into two parts: The first is a study of the RIP

near filling $\nu = 1/3$ using p-doped quantum wells, and the second is a zero-B-field study of ultra-dilute holes in undoped heterojunction-insulated-gate field-effect transistors (HIGFETs) at $r_s \geq 40$.

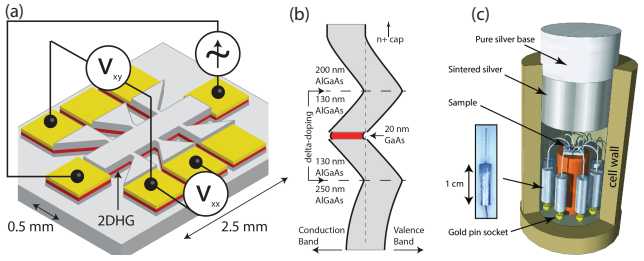

FIG. 1. (a) Sample dimensions and measurement configuration. (b) Band diagram of the quantum square well. (c) Cooling schematics inside a helium-3 immersion cell.

The samples used for the RIP measurement are lightly doped p-type (100) GaAs quantum wells patterned into a 2.5×0.5mm Hallbar. The density p is $\sim 4 \times 10^{10}$ cm^{-2} ($r_s = 24$), with mobility of $\mu \approx 2.5 \times 10^6$ cm^2/Vs. Thermally deposited AuBe pads annealed at 460 °C achieve excellent Ohmic contacts to the 2D carriers, with measured contact resistances $\sim$ 400 Ω. Measurements are performed in a dilution refrigerator inside a shielded room, allowing minimal electronic noises.

Cooling dilute carriers to 10 mK is challenging because sample thermalisation relies mainly on the cooling through the sample leads (via ee interaction) because the phonon modes are frozen out. We have established an effective cooling method via a helium-3 sample immersion cell and achieved 5 mK cooling GaAs 2D holes as dilute as $p = 5 \times 10^9$ cm^{-2} [30]. The carrier density for the RIP study here is nearly ten times higher. The cell is mounted at the lower end of a cold finger with its top fastened to the mixing chamber (mc) plate [Fig. 1(c)]. The roof is a sintered silver cylindrical-block extension made by compressed pure silver micro-particles. During operation, helium-3 gas is continuously fed through a capillary into the cell where it condenses to fill the volume completely. Saturated sintered silver block provides ∼30 m^2 contact area to cool the helium-3 bath. Major cooling of the 2D holes is realized via efficiently heat-sinking the metal contacts through sintered silver pillars providing 2.5 m^2 surface area per lead. T is monitored through a helium-3 melting curve thermometer. The T differential between the bath and the mc is ≤0.1mK at all times.

Fig. 2 (a) shows the magnetoresistance MR (ρ_{xx}) and the Hall resistance (ρ_{xy}) measured at 10 mK via a four-terminal ac technique. The inset shows the Shubnikov de Haas (SdH) oscillations starting at 0.05 T. The RIP peak centers at $B = 4.5$ T ($\nu = 0.375$) between fillings $\nu = 2/5$ and 1/3, with a dip in ρ_{xy} consistent with previous studies [31, 32]. $B = 4.5$ T corresponds to a magnetic length $l_B = \sqrt{hc/eB} \approx 28$nm equal to $a = 1/\sqrt{\pi p}$. This is where a WC is expected. However, we found that dc techniques, instead of the ac techniques, are the appropriate method probing the RIP peak because, as shown later, it is essential to measured bulk resistance r with currents of $\sim 1p$A which are far below the offset limits in the ac driving signals. An electrometer-level dc setup is therefore adopted with a voltage bias V between ±10mV (at 0.1μV resolutions). Current sensing via a low-noise preamp provides 50 fA precision.

Cooling to 9mK, dc-IV within a ±5nA window displays a sharp threshold [inset of Fig. 2(b)] apparently identical to a pinned CDW [33]. The differential resistance $r_d = dV/dI$ within the threshold $V_c \sim 1$me$V$ is approximately 1.3GΩ, with nearly no current flow ($I \leq 1-2p$A). This supports a collective pinning below a threshold electric field $E_c = V_c/L \sim 10m$V/cm because the single particle energy $w_c = eE_c a \sim 0.024\mu e$V (or 0.3 mK) is significantly smaller than T. $L \sim 0.5$mm is the distance between the voltage leads and $a = 1/\sqrt{\pi p} = 28n$m is the average charge spacing. However, current is switched on immensely at a critical current I_c and r_d plummets by nearly six thousands times. It indicates a phase transi-

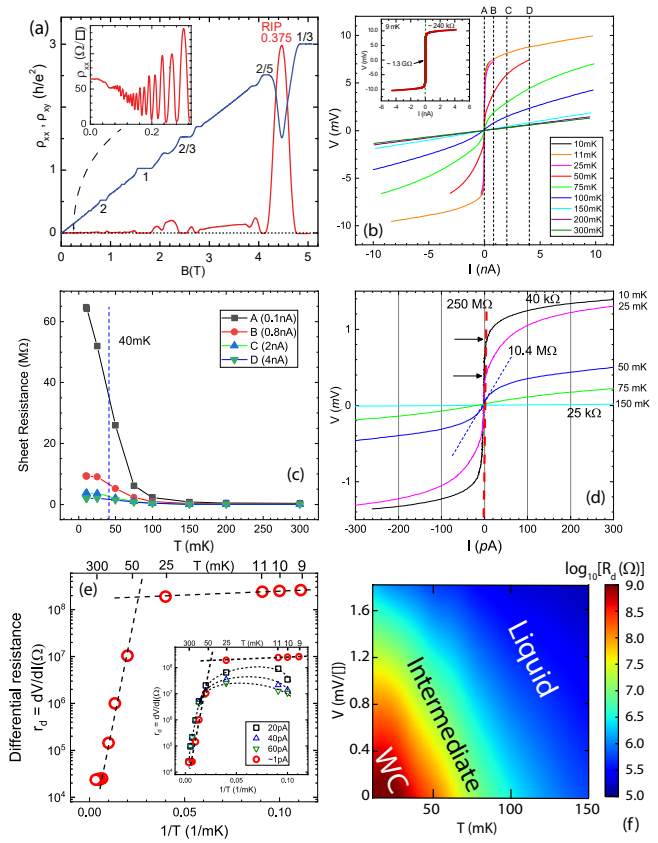

FIG. 2. (a) MR and Hall resistance at 10 mK. Inset: SdH oscillations. (b) dc-IV measured at B =4.5 T at various T from 10-300 mK. Inset: IV at 9mK. (c) T dependence of the resistance (V/I) measured with 0.1, 0.8, 2, and 4 nA driving currents. (d) Amplified view of (b) for a narrower current range. (e) Piecewise T dependence of $r_d(T) = dV/dI|_{V\to 0}$ on semi-logarithmic scales. Inset: comparison to $r_d(T)$ obtained with higher current drives. Dotted lines are guides. (f) Suggested contour phase diagram based on $\log_{10} R_d(T)$ values.

tion occurring at a remarkably small threshold current $I_c \sim 2p$A. This electric field (E)-driven phase transition becomes more evident in the later T dependent results. Joule heating is $< 10^{-15}$ Watts and thus negligible.

Another important evidence that supports a crystal phase is a melting transition which several studies have reported around 150-300mK [17–24, 27, 28, 34]. Fig. 2(b) shows IVs with each of the curves corresponding to a fixed T between 10 and 300 mK. The threshold behavior is robust up to ~ 40 mK, with $r_d \sim 1 - 1.3$GΩ and $I_c \sim 2 - 3p$A. For higher T, the threshold behavior is replaced with rounded nonlinear IVs between 40 and 140 mK with substantially suppressed $r_d \sim$MΩ. Eventually, linear IV is restored beyond 140 mK which is commonly recognized as a liquid phase due to the absence of pinning.

Naturally, a phase transition can be driven by both T and I (or V). Therefore, caution must be taken when examining the thermal melting because the sheet resistance $r = V/I$ are extremely sensitive to the level of the drives down to pA limits. For a demonstration, $r(T)$s obtained at four different randomly picked current drives, labeled by the dotted lines in Fig. 2(b), are plotted in Fig. 2(c). For $I \geq 1n$A, $r(T)$ varies little with increasing I, consistent with a liquid phase behavior. However, $r(T)$ exhibits more than two orders increase already with $I \sim 100p$A which must be linked to a transition effect.

Therefore, thermal melting must be examined in the limit of $I \to 0$. Fig. 2(e) shows $r_d(T)|_{I\to 0}$ in comparison to the $r_d(T)$ obtained at 20, 40 and 60 pA. $r_d(T)|_{I\to 0}$ is well described as a piece-wise behavior across a critical temperature of $\sim$ 35 mK defined as T_m. r_d decreases with increasing T at a rate of 1.5 MΩ/mK for $T \leq T_m$. For $T \geq T_m$, r_d exhibits an exponential dive marked by nearly four orders of magnitude down to 150 mK. The abrupt change within a few mK of T_m is referred to as a discontinuity that supports, also confirmed by the zero-field results shown later, a possible first order phase transition. The piecewise $r_d(T)$, however, disappears with I increased just beyond I_c. As shown in the inset of Fig. 2(e), $r_d(T)$ measured between 20 and 60 pA is substantially suppressed at $T \leq T_m$ and only smooth nonmonotonic crossovers are found. These results are consistent with what is indicated by the threshold behavior that a phase transition has occurred when $I > I_c$.

Meanwhile, though pinning at $T < T_m$ is consistently strong, V_c exhibits a noticeable T dependence. Fig. 2(d) shows selected IVs for 10, 25, 50, 75 and 150 mK within a narrower window. Note that r_d is now shown as resistivity (instead of resistance). For 10 and 25 mK, current switches on at different thresholds: 0.4 mV for 25 mK and 0.8 mV for 10 mK. Lower E_c for higher T is qualitatively consistent with the Lindemann criterion for crystal melting [15]. An estimate of ξ is provided here, similar to previous studies [19, 35], based on a pinning model [36, 37] that balances the pinning energy with the electrical potential energy $U = Nw_c$. $w_c = eE_c a \sim 0.024\mu$eV$\ll T$ is the single particle potential energy. $N = p\xi^2$ is the number of carriers on a scale of ξ. For $T = 25m$K, $E_c = V_c/L \sim 8\ mV/$cm where $L = 0.5$ mm. Setting the electrical force NeE_c equal to the pinning force κa [18, 19], κ being the shear modulus $0.245e^2p^{3/2}/4\pi\epsilon_0\epsilon$ [38], $N \sim 1.5 \times 10^5$ or $\xi \geq 10\mu$m is obtained. U is $\sim 2.4m$eV (or 30 K), comparable to E_{ee}.

For T between 40 and 140 mK, the threshold is replaced with a rounded nonlinear IV. This observation is in agreement with several previous results [18, 27, 28, 34] which were interpreted as pinned WCs. However, E_c disappears because a current switches on in the limit of $V \to 0$. In addition, pinning is substantially reduced, i.e. $r_d \sim 10$MΩ at 50 mK. Therefore, this region should be of an intermediate phase since it crosses over to a liquid above 140 mK (referred to as T_l). r_d for $T \geq T_l$ is 30-40 k$\Omega/\square$. The same values of r_d are found for the liquid phase arrived by E-field-driven melting at sufficiently large bias. A suggested phase diagram is shown in Fig. 2(f).

To identify the nature of the intermediate phase is difficult because the exact relationship between r_d and $\xi(T)$ has to be first formulated. Here, as a minor point, we show that $r_d(T)$ can be fitted to $r_d = r_0 \exp[c/(T - 40mK)^\gamma]$ with $r_0 \approx 23$ and $c \approx 9.5$, in the same trend as the exponentially decreasing $\xi(T)$ modeled for a hexatic phase [13]: $\xi \sim \exp[c/(T - T_m)^\gamma]$ ($\gamma \approx 0.3696$).

We now turn to the zero-B-field study with undoped GaAs/AlGaAs HIGFETs [39–41]. A 6 mm$\times$0.8 mm Hall-bar is realized with a self-align fabrication process [41] [Fig. 3(a)]. Accumulation of holes at the hetero-interface is capacitively induced through biasing a top gate beyond a turn-on voltage, ~ -1.3 V, at which the valance band edge meets the chemical potential [Fig. 3(b)]. The band gap of the 600nm-thick $Al_{0.3}Ga_{0.7}As$ barrier is $\sim$2 eV. Owning to the superior crystal quality, gate leakage remains less than 0.05 pA at all operating bias. Density p, determined via quantum Hall oscillations [Fig. 3(c)], is tunable from 4×10^{10} down to 7×10^8 cm^{-2}.

Accessing $r_s \geq 40$ requires $p \leq 4 \times 10^9$ cm^{-2}. $m^* = 0.25m_0$ is a lower-bound estimate. [Determination of m^* is difficult because of a complicated dispersion relation associated with the light-heavy hole bands mixing and the spin-orbit coupling [42].] It is thus important to exclude disorder-driven localization which easily occurs as phonon-activated hopping $\rho(T) \sim \rho_0 \exp(-T^*/T)^{1/\beta} (\beta = 1 - 3)$ [43, 44]. Recent studies of ultra-clean systems revealed nonactivated power-law behaviors [40, 45, 46] of interaction-driven nature that dis-

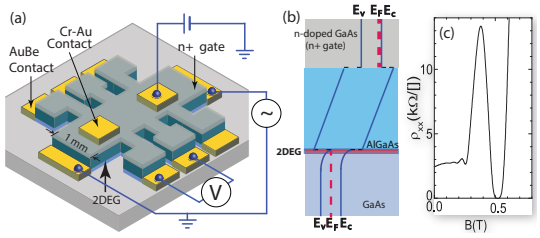

FIG. 3. (a) HIGFET sample and measurement schematics. (b) Band diagram showing accumulation of holes at the GaAs/AlGaAs junction. (c)$\rho_{xx}(B)$ for $p = 1.2 \times 10^{10}$ cm^{-2}.

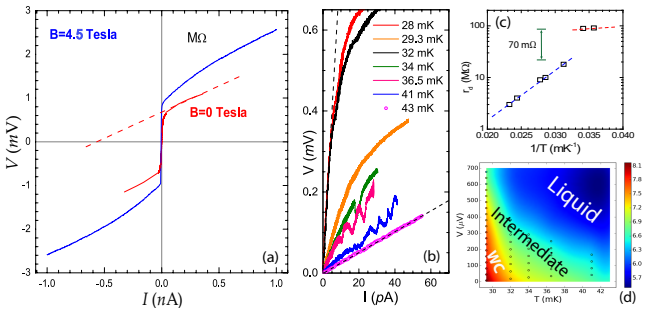

FIG. 4. (color online) (a) dc-IV at T =28 mK. (b) IVs obtained at different T. (c) T dependence of $r_d(T)|_{V\to 0}$ on semi-logarithmic scales. (d) Colored contour phase diagram based on $\log_{10} R_d(T)$ values. Dashed lines are guides.

tinguishes from a disorder-driven effect. And, the metal-to-insulator transition (MIT) [47] occurs at lowest carrier densities corresponding to $r_s \sim 35-40$. We refer the readers to references [40, 45, 46, 48] for details.

The measured MIT in zero-B (not shown) has a critical density $p_c = 4\times 10^9$ cm^{-2}. The following dc results are for $p = 2.8\times 10^9$ cm^{-2} (or $r_s \sim 45$) measured between 28 to 45 mK. A current bias, with Keithley 6430 fA source, is employed with a voltage sensing at sub-μV-resolution at an input impedance of $10^{16}\Omega$. Fig.4(a) shows a similar threshold IV obtained at 28 mK qualitatively identical to the RIP case. $I_c \sim 4p$A. Strong sub-threshold pinning is marked by a r_d of 90 M$\Omega/\Box$. The supra-threshold r_d collapses one hundred times. I_c corresponds to a $E_c \sim 4m$V/cm (or $\sim 10^{-10}$ V/a_B), yielding a slightly larger single particle potential energy of $\sim eE_ca \sim 0.04\mu eV$ (or 0.46 mK) due to the larger $a \sim 100$ nm. Setting $NeE_c = \kappa a$ as shown earlier, one obtains $N \sim 1\times 10^5$, corresponding to a substantial scale of $\xi \sim 100\mu$m. This yields a dominating potential energy $U \sim 20m$eV $> E_{ee}$ which is consistent with a crystal. For a consistency check, the same setup is used to measure the RIP and the result is shown as the blue curve. The power dissipation is $\leq 2\times 10^{-16}$ Watts, ruling out appreciable Joule heating.

Melting probed by $r_d|_{I\to 0}$ is shown in Fig. 4(c) where a piecewise behavior appears across $T_m \sim 30$ mK. dr_d/dT is 4MΩ/mK for $T < T_m$. r_d exhibits a discontinuous jump of 70MΩ at T_m above which an exponential T dependence is found. E_c disappears at $T > T_m$ where rounded nonlinear IV is found. The discontinuous jump resembles a recent quantum Monte Carlo simulation for a first order WC-intermediate phase transition mediated by a discontinuous internal energy jump [10], and supports a singularity dividing a WC from an intermediate phase. Linear IV is recovered at $T_l \sim 42$ mK, noticeably lower than the RIP case. Smaller T_m and T_l for the ultra-dilute case is qualitatively consistent with stronger quantum fluctuations and disorder fluctuations (due to lack of screening). A phase diagram is suggested in Fig. 4(d).

Increasing E-field results in a switch-on of current and a settlement of r_d belonging to a liquid phase. Identical to the RIP case, a melting mediated by an intermediate phase is supported. However, there is a noticeable difference in the intermediate phase at $T > T_m$: V oscillates with increasing I at approximately 5-10 pA spacing. It occurs more frequently as T approaches T_l [Fig. 4(b)]. The formation of stripes with long-range orientational order [13], as seen in electrons on a helium surface [49], could be a possible cause. Another possibility is that small T_l facilitates a melting and re-crystallization of pinned WC domains, instead of or in addition to shearing, when driven across pinning sites [50]. This will contribute to a negative r_d.

To summarize, enormous pinning modes below T_m supports a WC on large ξ scales. A melting is captured as a two-stage SLT. The WC-intermediate phase transition is likely first-ordered [14] because of the discontinuity in r_d as well as the disappearance of E_c above T_m. Results obtained from both RIP and zero-B-field studies are remarkably consistent. The small T_m, which is $\sim (1/7)T_{cm}$, suggests strong effects from system disorders and quantum fluctuations that require further understanding.

This work is supported by NSF under DMR-1410302, and by the Gordon and Betty Moore Foundation through Grant GBMF2719, and NSF MRSEC-DMR-0819860.

[1] E. Wigner, Phys. Rev. **46**, 1002 (1934).
[2] N. D. Mermin and H. Wagner, Phys. Rev. Lett. **17**, 1133 (1966).
[3] N. D. Mermin, Phys. Rev. **176**, 250 (1968).
[4] J. Kosterlitz and D. Thouless, Journal of Physics C: Solid State Physics **5**, L124 (1972).
[5] B. Tanatar and D. M. Ceperley, Phys. Rev. B **39**, 5005 (1989).
[6] P. W. Anderson, Phys. Rev. **109**, 1492 (1958).
[7] H. Aoki, Journal of Physics C: Solid State Physics **12**, 633 (1979).
[8] P. Anderson, *Basic Notions of Condensed Matter Physics* (Benjamin/Cummings, Menlo Park, California, 1984).
[9] M. Takahashi and M. Imada, Journal of the Physical Society of Japan **53**, 3765 (1984), http://dx.doi.org/10.1143/JPSJ.53.3765.
[10] B. K. Clark, M. Casula, and D. M. Ceperley, Phys. Rev. Lett. **103**, 055701 (2009).
[11] J. M. Kosterlitz and D. J. Thouless, Journal of Physics C: Solid State Physics **6**, 1181 (1973).
[12] B. I. Halperin and D. R. Nelson, Phys. Rev. Lett. **41**, 121 (1978).
[13] D. R. Nelson and B. I. Halperin, Phys. Rev. B **19**, 2457 (1979).
[14] B. K. Clark, M. Casula, and D. M. Ceperley, Phys. Rev. Lett. **103**, 055701 (2009).
[15] G. M. Bruun and D. R. Nelson, Phys. Rev. B **89**, 094112 (2014).
[16] A. P. Young, Phys. Rev. B **19**, 1855 (1979).
[17] H. W. Jiang, H. L. Stormer, D. C. Tsui, L. N. Pfeiffer,

and K. W. West, Phys. Rev. B **44**, 8107 (1991).
[18] V. J. Goldman, M. Santos, M. Shayegan, and J. E. Cunningham, Phys. Rev. Lett. **65**, 2189 (1990).
[19] F. I. B. Williams, P. A. Wright, R. G. Clark, E. Y. Andrei, G. Deville, D. C. Glattli, O. Probst, B. Etienne, C. Dorin, C. T. Foxon, and J. J. Harris, Phys. Rev. Lett. **66**, 3285 (1991).
[20] E. Y. Andrei, G. Deville, D. C. Glattli, F. I. B. Williams, E. Paris, and B. Etienne, Phys. Rev. Lett. **60**, 2765 (1988).
[21] Y. P. Chen, G. Sambandamurthy, Z. H. Wang, R. M. Lewis, L. W. Engel, D. C. Tsui, P. D. Ye, L. N. Pfeiffer, and K. W. West, Nat Phys **2**, 452 (2006).
[22] H. Zhu, Y. P. Chen, P. Jiang, L. W. Engel, D. C. Tsui, L. N. Pfeiffer, and K. W. West, Phys. Rev. Lett. **105**, 126803 (2010).
[23] M. A. Paalanen, R. L. Willett, P. B. Littlewood, R. R. Ruel, K. W. West, L. N. Pfeiffer, and D. J. Bishop, Phys. Rev. B **45**, 11342 (1992).
[24] J. Jang, B. M. Hunt, L. N. Pfeiffer, K. W. West, and R. C. Ashoori, Nature Physics (2016).
[25] D. R. Nelson and B. I. Halperin, Phys. Rev. B **21**, 5312 (1980).
[26] S. V. Kravchenko, J. A. A. J. Perenboom, and V. M. Pudalov, Phys. Rev. B **44**, 13513 (1991).
[27] V. M. Pudalov, M. D'Iorio, S. V. Kravchenko, and J. W. Campbell, Phys. Rev. Lett. **70**, 1866 (1993).
[28] J. Yoon, C. C. Li, D. Shahar, D. C. Tsui, and M. Shayegan, Phys. Rev. Lett. **82**, 1744 (1999).
[29] M. Y. Simmons, A. R. Hamilton, M. Pepper, E. H. Linfield, P. D. Rose, D. A. Ritchie, A. K. Savchenko, and T. G. Griffiths, Phys. Rev. Lett. **80**, 1292 (1998).
[30] J. Huang, J. S. Xia, D. C. Tsui, L. N. Pfeiffer, and K. W. West, Phys. Rev. Lett. **98**, 226801 (2007).
[31] T. Sajoto, Y. P. Li, L. W. Engel, D. C. Tsui, and M. Shayegan, Phys. Rev. Lett. **70**, 2321 (1993).
[32] M. Hilke, D. Shahar, S. Song, D. Tsui, Y. Xie, and D. Monroe, Nature **395**, 675 (1998).
[33] G. Grüner, Rev. Mod. Phys. **60**, 1129 (1988).
[34] S. V. Kravchenko, J. A. A. J. Perenboom, and V. M. Pudalov, Phys. Rev. B **44**, 13513 (1991).
[35] V. J. Goldman, M. Shayegan, and D. C. Tsui, Phys. Rev. Lett. **61**, 881 (1988).
[36] P. A. Lee and H. Fukuyama, Phys. Rev. B **17**, 542 (1978).
[37] H. Fukuyama and P. A. Lee, Phys. Rev. B **17**, 535 (1978).
[38] L. Bonsall and A. Maradudin, Physical Review B **15**, 1959 (1977).
[39] B. E. Kane, L. N. Pfeiffer, and K. W. West, Applied Physics Letters **67**, 1262 (1995).
[40] H. Noh, M. P. Lilly, D. C. Tsui, J. A. Simmons, E. H. Hwang, S. Das Sarma, L. N. Pfeiffer, and K. W. West, Phys. Rev. B **68**, 165308 (2003).
[41] J. Huang, D. S. Novikov, D. C. Tsui, L. N. Pfeifer, and K. W. West, International Journal of Modern Physics B **21**, 1219 (2007).
[42] R. Winkler, *Spin–Orbit Coupling Effects in Two-Dimensional Electron and Hole Systems* (Springer, 2003).
[43] N. F. Mott, Philosophical Magazine **19**, 835 (1969), http://dx.doi.org/10.1080/14786436908216338.
[44] A. L. Efros and B. I. Shklovskii, Journal of Physics C: Solid State Physics **8**, L49 (1975).
[45] J. Huang, D. S. Novikov, D. C. Tsui, L. N. Pfeiffer, and K. W. West, Phys. Rev. B **74**, 201302 (2006).
[46] J. Huang, L. N. Pfeiffer, and K. W. West, Phys. Rev. B **85**, 041304 (2012).
[47] S. V. Kravchenko, W. E. Mason, G. E. Bowker, J. E. Furneaux, V. M. Pudalov, and M. D'Iorio, Phys. Rev. B **51**, 7038 (1995).
[48] J. Huang, L. N. Pfeiffer, and K. W. West, Phys. Rev. Lett. **112**, 036803 (2014).
[49] P. Glasson, V. Dotsenko, P. Fozooni, M. J. Lea, W. Bailey, G. Papageorgiou, S. E. Andresen, and A. Kristensen, Phys. Rev. Lett. **87**, 176802 (2001).
[50] B. Normand, P. Littlewood, and A. Millis, Physical Review B **46**, 3920 (1992).